

Turbo: Informativity-Driven Acceleration Plug-In for Vision-Language Models

Chen Ju^{1*}, Haicheng Wang^{1*}, Zeqian Li¹, Xu Chen², Zhonghua Zhai², Weilin Huang², Shuai Xiao²

¹ CMIC, Shanghai Jiao Tong University ² TAO Technology, Alibaba Group

{ju.chen, anakin_skywalker, lzq0103}@sjtu.edu.cn

{huaisong.cx, zhaizhonghua.zzh, weilin.hwl, shuai.xsh}@taobao.com

Abstract

Vision-Language Large Models (VLMs) have become primary backbone of AI, due to the impressive performance. However, their expensive computation costs, i.e., throughput and delay, impede potentials in real-world scenarios. To achieve acceleration for VLMs, most existing methods focus on the model perspective: pruning, distillation, quantification, but completely overlook the data-perspective redundancy. To fill the overlook, this paper pioneers the severity of data redundancy, and designs one plug-and-play Turbo module guided by information degree to prune inefficient tokens from visual or textual data. In pursuit of efficiency-performance trade-offs, information degree takes two key factors into consideration: mutual redundancy and semantic value. Concretely, the former evaluates the data duplication between sequential tokens; while the latter evaluates each token by its contribution to the overall semantics. As a result, tokens with high information degree carry less redundancy and stronger semantics. For VLMs' calculation, Turbo works as a user-friendly plug-in that sorts data referring to information degree, utilizing only top-level ones to save costs. Its advantages are multifaceted, e.g., being generally compatible to various VLMs across understanding and generation, simple use without retraining and trivial engineering efforts. On multiple public VLMs benchmarks, we conduct extensive experiments to reveal the gratifying acceleration of Turbo, under negligible performance drop.

1. Introduction

Vision-Language Large Models (VLMs) [12, 21–23, 31] have achieved promising progress towards artificial intelligence. Inspired by superior performance and emergent abilities, VLMs are even considered as one of the future trend towards AGI. As some studies [4, 45] illustrated, VLMs' capability is closely linked to two core factors: model parameters and data quality. Therefore, expanding the model scale and feeding high-quality data to improve the prac-

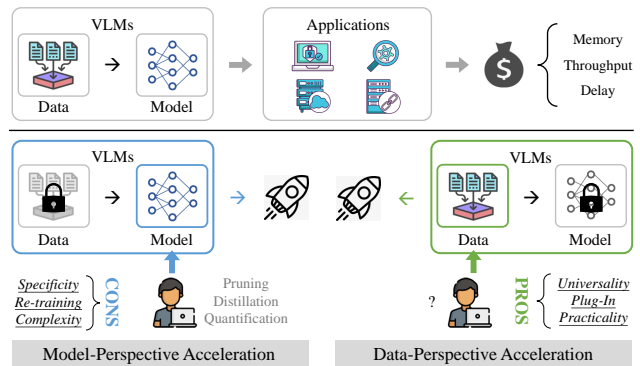


Figure 1. **Top.** The trouble for VLMs in implementation is the cost issue: memory and throughput. **Bottom.** Most ideas focus on the model-perspective acceleration, i.e., pruning & quantification. Our Turbo explores data-perspective acceleration by de-redundancy.

tical performance, has become the community consensus. As expected, VLMs demonstrates superior results on various downstream tasks/domains [14, 34, 48], including understanding and generation, with delicate architectures.

Although it seems that building leading to AI has been completed, there is still a dark cloud hanging over VLMs, making everything a utopia. That is, the cost issue (computational throughput/latency/memory), whether it is training or deployment. Let's imagine, for text-to-image generation, the snail's pace of one picture every 10 seconds is a bottleneck for real-world applications. As a result, reducing costs becomes key to promoting the popularity of VLMs.

To achieve acceleration for VLMs, most existing methods focus on **one Model-Center Perspective (MCP)** [35, 43], e.g., pruning, distillation, quantification, as shown in Figure 1. Although effective, they have three following issues: **Specificity.** MCP is only developed for specific network architectures with poor generalization, which means it's incompatible with various VLMs. For example, MCP acceleration suitable for understanding is usually infeasible for generation. **Re-training.** In order to maintain high performance, MCP usually requires re-training or fine-tuning VLMs, which inevitably consumes additional computing

overheads, *i.e.*, being inefficient to apply. **Complexity.** The development of MCP involves considerable tricks, these trivial matters raises barriers to applications. To sum up, MCP is trapped in one dilemma: easy to hit ceiling, as well as hard to be generalized.

To jump out of the dilemma, this paper raises one novel question about acceleration, from **one Data-Center Perspective (DCP)**: Is there redundancy in the data? And if so, how high? To take one step answering the question, we first define, then evaluate the informativity of token sequences in each VLMs block. The exploration motivation is that attention-based networks have emerged as a dominant architecture among VLMs, resulting in a quadratic relationship between computation and input sequence length. Results show, token redundancy is consistently high in most blocks. Besides, token redundancy gradually increases as blocks deepen. With these observations, we conclude that acceleration through data de-redundancy is promising.

To enable data acceleration, we propose one novel Turbo plug-in module, with the spirit that compressing invalid components while retaining semantic essences. Concretely, we define an information degree, covering two components: mutual redundancy and semantic value. The former evaluates the information duplication between sequential tokens, while the latter focuses on the token’s contribution to sample-wise semantics. For mutual redundancy, the insight is that tokens with dependency tend to have similar informativity, making re-use feasible. For semantic value, the insight is that tokens with core contributions maintain strong performance as principal components. Using information degree of sequential tokens, Turbo naturally sorts data to only leverage the top-level ones for VLMs’ calculation, thus saving costs from the source. To sum up, Turbo wins considerable pros. **Universality.** The accelerated data could directly compatible with on various VLMs, *e.g.*, understanding/generation, multi-modality/uni-modality, showing the powerful generalization. **Plug-and-Play.** Turbo involves no training parameters, which is lightweight to avoid trivial development efforts. **Practicality.** Turbo is user-friendly with no tedious tricks. Even more valuable, it can complement existing model-perspective acceleration.

Under two types of VLMs, namely, image-align-text understanding and text-to-image generation, we conduct experiments to prove the acceleration generality of Turbo, across several standard datasets. For almost all understanding tasks (retrieval, classification, caption and VQA), Turbo improves throughput by around 2X with little loss of performance. For most generation tasks (text-to-image, image-to-image), Turbo improves throughput to 1.6X without compromising quality. We do extensive ablations to reveal the component effectiveness, both quantitatively and qualitatively. Comparing to existing acceleration ideas, Turbo gets better efficiency-performance trade-offs, showing great po-

tential for resource-constrained scenarios.

To sum up, our contributions lie in three folds:

- We pioneer a data-perspective acceleration for VLMs, by token de-redundancy, which is universally adapted to any attention-based understanding and generation models.
- We design one novel Turbo plug-in to perform data de-redundancy by information degree of redundancy and semantics, getting great efficiency-performance trade-offs.
- We conduct extensive experiments and thorough ablations to reveal the great significance of Turbo acceleration, and our superior results on understanding/generation tasks.

2. Related Work

Vision-Align-Language Understanding learns image-text shared embedding spaces, by pre-training with large-scale data. The recent studies mainly divided into three groups, namely, single tower [6,21], twin towers [12,31], and bridge tower [22,23,49]. Structurally, attention-based Transformer has emerged as a dominant architecture, greatly increasing computing overhead while improving performance. They have brought many promising potentials in terms of understanding videos [17–19], audio [24, 26] and image [5, 7]. More specifically, it can be broken down into the following tasks: recognition [20, 47], grounding [16, 25], segmentation [29, 46], caption [27, 30], retrieval [14, 40].

Vision-Language Generation aims to build compositional models from text & noise to pixel-wise vision. Typically, research lines are mainly divided into: Diffusion (SD) [11, 34] and DALL-E [32, 38]. Although they have shown promising potentials [15, 28], expensive computing costs seriously damage user experience. For instance, when using SD for one 1024 * 1024 image, the inference delay is about 8 seconds. Structurally, SD’s UNet accounts for most overhead.

Acceleration for VLMs. To cut high computing costs, extensive work has been proposed to accelerate VLMs, for deployment on resource-limited devices. To sum up, there are four main ideas, namely, knowledge distillation [9, 43], floating quantification [35], and model pruning [33, 36, 43] and retraining for data pruning [13, 37, 44]. Although these methods achieve high sparsity with competitive performance, they all suffer from the model-perspective dilemma, in the following aspects. *Re-training.* To maintain high performance, fine-tuning VLMs is usually inevitable, which is inefficient to consume additional computing overheads. *Specificity.* They are generally developed for specific network architectures, which have poor generalization to compatible with various VLMs. *Complexity.* They could involve many tricks in empirical, these trivial matters raises barriers to application. Overall, comparing to above methods, our Turbo is totally training-free, can be easily plugged in most VLMs with the competitive performance.

Recently, ToMe [2] is been proposed as an acceleration plug-in, but Turbo differs from it in two aspects. **Universal-**

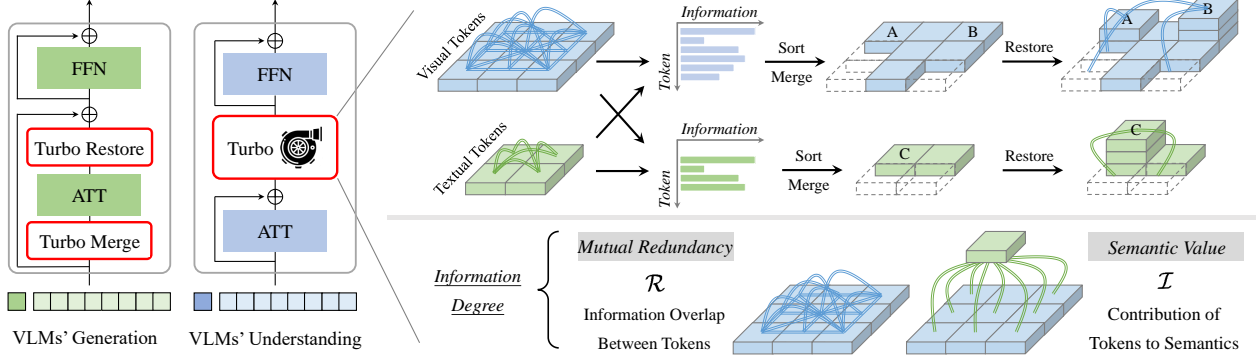


Figure 2. **Computing Architecture.** As a plug-in module, Turbo calculates information degree (mutual redundancy and semantic value) to sort the VLMs’ tokens, and then merges tokens for data reduction. It shows strong generalization across understanding/generation and uni-modality/multi-modality, and is flexible to apply in any block of VLMs to cut computation overheads.

ity. ToMe works only for uni-modal image classification; while Turbo is generally compatible to various VLMs: understanding/generation, multi-modality/uni-modality. **All-round.** ToMe focuses solely on mutual redundancy; while Turbo combines mutual redundancy and semantic value, to achieve better acceleration-performance trade-offs.

3. Acceleration for VLMs

With the goal of alleviating heavy deployment costs from VLMs, we conduct thorough analysis in terms of data; then describe informativity-driven turbo plug-in for acceleration.

3.1. Preliminaries

Revisit of Attention. For VLMs, Transformer composed of attention has emerged as a dominant architecture. For either text or image data, we generally processes it as the N -token 1D sequence $\mathbf{X} \in \mathbb{R}^{N \times D}$, then pass into the attention layer to model sequence relationships globally, where one weighted sum of values based on the affinity over other tokens is calculated. Formally, attention is formulated as:

$$\text{Attention}(\mathbf{Q}, \mathbf{K}, \mathbf{V}) = \text{softmax}\left(\frac{\mathbf{Q}\mathbf{K}^T}{\sqrt{D}}\right)\mathbf{V}, \quad (1)$$

Transformer achieves impressive performance compared to previous architectures, *e.g.*, convolution and graph, but at the cost of being more expensive. It’s because the complexity of multi-head attention modules (self-attention or cross-attention) scales quadratically with the sequence length N , long tokens lead to substantial computational overheads.

With the fundamental understanding, we raise one novel question: Is there any redundancy in the token sequence? If so, we can remove such redundancy from one data perspective, to cut off computational overheads from the source.

3.2. Multi-Modal Information Redundancy

Motivation & Insight. Given that most input data are likely to contain superfluous parts, *e.g.*, image background, irrelevant objects, we foresee a significant opportunity to further compress the data. In order to accelerate the inference from data perspective, the primary process is to distinguish where the redundancy lies. To analyse it quantitatively, we define token sequence informativity as a measure to quantify the information contained in one token sequence.

Inspired by the informativity idea in information theory, we define $(\Omega, \mathcal{F}, \mathbb{P})$ as the probability space of token sequences, where the triplet is sample space, σ -algebra and probability measure respectively. For one token sequence $\mathbf{X} = [x_1, x_2, \dots, x_n]$, we define its informativity as:

$$\mathcal{I}(\mathbf{X}) = -\log \mathbb{P}(\mathbf{X}) = -\log \mathbb{P}([x_1, x_2, \dots, x_n]), \quad (2)$$

By the compound probability formula, we have

$$\mathcal{I}(\mathbf{X}) = -\log \mathbb{P}(x_{k,k \in \psi} | x_{i,i \in \{\phi - \psi\}}) \cdot \mathbb{P}(x_{i,i \in \{\phi - \psi\}}), \quad (3)$$

where $\phi = \{1, \dots, n\}$ and ψ is a subset of ϕ . If we manage to find a subset ψ such that

$$\mathbb{P}(x_{k,k \in \psi} | x_{i,i \in \{\phi - \psi\}}) \approx 1 \quad (4)$$

then sequence informativity can be approximated by

$$\mathcal{I}(\mathbf{X}) \approx -\log \mathbb{P}(x_{i,i \in \{\phi - \psi\}}). \quad (5)$$

This approximation demonstrates that if we manage to find a subset of token sequence $\{x_{k,k \in \psi}\}$ which have a total dependency on its complementary set $\{x_{i,i \in \{\phi - \psi\}}\}$, then we could aggregate $\{x_{k,k \in \psi}\}$ into its complementary set for more efficient calculation without much information loss.

Mutual Redundancy. According to the above analysis, we would like to find the dependencies between tokens of the

given sequence. MAE [10] shows that there exists considerable redundancies in image tokens, such that only 25% tokens can almost restore the whole sequence, thus a such subset ψ is verified to exist. However, it’s nontrivial to find a proper subset, for the token dependencies is unknown.

One intuition is that tokens with mutual dependency tend to have similar representations, *e.g.*, we could easily restore the texture of a shirt by just a few patches from it. What’s more, notice that tokens with high similarity have analogical contributions in the attention calculation. As some studies [2] have shown, token aggregation by mutual similarity is able to preserve key information. So by pairing up tokens with similar representations, we manage to construct a subset $\{x_{k,k \in \psi}\}$ with a high dependency on $\{x_{i,i \in \{\phi-\psi\}}\}$.

Semantic Value. Mutual redundancy for data pruning can already get relatively good results on simple tasks, *i.e.*, image classification. However, in this process, each token is treated equally, thus its contribution to semantic categories are neglected. This will result in an early merging for tokens with important semantics, causing a drastic performance drop on fine-grained, information-demanding tasks, *i.e.*, multi-modal understanding and generation.

To merge tokens with a preference from trivial background to significant foreground, we leverage the guidance of semantic value hidden inside the network. We consider *cls* token as the semantic enrichment. For *cls* token \mathbf{Y} , we can calculate its informativity as:

$$\mathcal{I}(\mathbf{Y}) = -\log \mathbb{P}(\mathbf{Y}) = -\log \mathbb{P}(\mathbf{A} \cdot \mathbf{V}), \quad (6)$$

where \mathbf{V} is the affine transformation of token sequence \mathbf{X} , and \mathbf{A} refers to the attention map for the *cls* token:

$$\mathbf{A} = \text{softmax}\left(\frac{\mathbf{Q}_{\text{cls}} \mathbf{K}^T}{\sqrt{D}}\right) \in \mathbb{R}^{1 \times n}, \sum_{i=1}^n \mathbf{A}_{1,i} = 1. \quad (7)$$

We define the **semantic value** of i -th token as its attention weight $A_{1,i}$. As we have no access to the probability distribution of \mathbf{V} , here we adopt one meandering way to approximate the solution. Inspired by vector quantization [8, 42], one common sense can be summarized as follows. In the context of neighbourhood, continuous variables can be approximately represented by discrete quantities, which illustrate the fact that if we place the perspective in a local neighborhood, vectors that are closer in distance tend to possess similar semantic meanings. Thus we make a first-order approximation that under the condition of neighbourhood near semantic-rich $y_1 \in R^n$ with range $\epsilon > 0$, for all $y_2 \in R^n$ satisfying $\|y_1 - y_2\|_2 < \epsilon$, there exists an $\beta \in R_+$ so that

$$\|\mathcal{I}(y_1) - \mathcal{I}(y_2)\| \leq \beta \|y_1 - y_2\|_2. \quad (8)$$

Denote \mathbf{Y}' the *cls* token after pruning the tokens $\{x_{j,j \in \psi'}\}$,

with $\psi' \subseteq \{1, \dots, n\}$:

$$\mathbf{Y}' = \sum_{i=1}^n \mathbf{A}_i \mathbf{V}_i - \sum_{j \in \psi'} \mathbf{A}_j \mathbf{V}_j = \mathbf{A}' \cdot \mathbf{V}', \quad (9)$$

Replacing y_1 by the original *cls* token \mathbf{Y} and y_2 by the pruned *cls* token \mathbf{Y}' in Eq. 8:

$$\|\mathcal{I}(\mathbf{A} \cdot \mathbf{V}) - \mathcal{I}(\mathbf{A}' \cdot \mathbf{V}')\| \leq \beta \|\mathbf{A} \cdot \mathbf{V} - \mathbf{A}' \cdot \mathbf{V}'\|_2. \quad (10)$$

Suppose we have

$$\left\| \sum_{j \in \psi'} \mathbf{A}_j \mathbf{V}_j \right\|_2 \ll \frac{1}{\beta}, \quad (11)$$

With the prior assumption in Eq. 8, we can approximate the informativity of *cls* token $\mathcal{I}(\mathbf{Y})$ as $\mathcal{I}(\mathbf{Y}')$ because

$$\|\mathcal{I}(\mathbf{Y}) - \mathcal{I}(\mathbf{Y}')\| \leq \beta \left\| \sum_{j \in \psi'} \mathbf{A}_j \mathbf{V}_j \right\|_2 \ll 1. \quad (12)$$

Such theoretical analysis indicates that, pruning/merging tokens with sufficiently small semantic values, will barely affect the informativity of *cls* token.

Semantic value captures token importance/relevance to the overall semantics. We add it into the merging strategy, giving tokens with high semantics less weight during the reduction. This ensures that tokens with high semantic contributions are more likely to be retained, even if their mutual redundancy is high. Figure 4 and Section 4.3 implies the mentioned properties of semantic value.

Remark. For uni-modal tasks, we adopt visual *cls* token as semantic guidance; while for multi-modal tasks, we use visual or textual *cls* token depending on model architectures.

3.3. Empirical Evaluation of Redundancy

As proposed above, we identify mutual redundancy and semantic value as the two main sources of redundancy in the inference process. To quantitatively measure these redundancies in the output token sequence $\mathbf{X} = [\mathbf{x}_1, \mathbf{x}_2, \dots, \mathbf{x}_n]$ of one attention layer, we first define evaluation metrics for mutual redundancy, named as token redundancy, *i.e.*, measure cosine similarities \mathcal{S} between tokens:

$$\mathcal{S} = \frac{2}{n * (n - 1)} \sum_{i=1}^n \sum_{j=i+1}^n \frac{\mathbf{x}_i \cdot \mathbf{x}_j}{\|\mathbf{x}_i\|_2 \|\mathbf{x}_j\|_2}, \quad (13)$$

where $\|\cdot\|_2$ is the L2 norm and \cdot is the dot product.

Then we define the attention concentration \mathcal{C} as the proportion of semantic values in the top $\frac{1}{4}$ tokens with highest values:

$$\mathcal{C} = \sum_{i=1}^{\lfloor \frac{n}{4} \rfloor} \mathbf{A}_{1,i}, \quad (14)$$

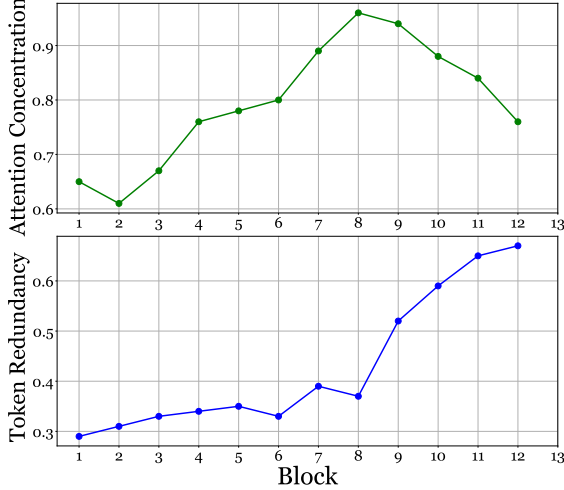


Figure 3. **Empirical Evaluation of Redundancy.** We experiment on BLIP image encoder fine-tuned for multi-modal retrieval. The results support our argument for potential redundancies in data.

where \mathbf{A} is the semantic value defined in Eq. 7. We use this measure to verify the long-tail distribution of semantic values. Larger \mathcal{C} implies a higher degree of concentration on few specific tokens, encouraging safe reduction to insignificant trailing tokens without losing much information.

To view underlying redundancies in VLMs, we experiment on image encoder of BLIP [23], with the parameters fine-tuned on COCO retrieval datasets. Figure 3 counts token redundancy and attention concentration. By analyzing results, we empirically draw the following conclusions:

- **Basis:** token redundancy and attention concentration are consistently high in most blocks, achieving 95% in intermediate layers, *i.e.*, the left $\frac{3}{4}$ tokens contributes only 5%.
- **Trend:** token redundancy gradually increases as blocks deepen, implying a tendency of clustering done by the network. Attention concentration presents a bottleneck trend, with the maximum value reached at the intermediate layer.

These above observations support the fact that tokens in the attention layer possess high mutual redundancy and concentrated semantic values, thus acceleration by data de-redundancy is promising. We next achieve the goal by one novel Turbo plug-in.

3.4. Plug-and-Play Turbo

Strategy. Information degree \mathcal{E} is proposed to balance mutual redundancy \mathcal{R} and semantic value \mathcal{I} , we explore two fusion strategies: weighted averaging or coupled product.

$$\mathcal{E} = \mathcal{R} - \alpha\mathcal{I}, \quad \mathcal{E} = \frac{\mathcal{R}}{\mathcal{I}}. \quad (15)$$

Table 7 makes detailed comparisons, and shows the significance of trade-offs between \mathcal{R} and \mathcal{I} .

With information degree \mathcal{E} , we naturally propose a Turbo module to accelerate by data de-redundancy. Since the data organization of most VLMs is attention-based sequences, Turbo could perform on any block with great flexibility.

Role. Structurally speaking, Turbo does behave in differentiated forms for generation and understanding.

For high-level semantic tasks (such as, classification, retrieval, caption, VQA), the role of Turbo is to calculate the information degree for N input tokens $\mathbf{X} \in \mathbb{R}^{N \times D}$, and then sort them to merge the top-level ones to the rest \mathbf{X}' . Formally:

$$\mathbf{X}' = \Phi_{\text{tub}}^{\text{high}}(\mathbf{X}, \Upsilon) \in \mathbb{R}^{N \cdot (1-\Upsilon) \times D} \quad (16)$$

where Υ is the token drop ratio to all sequential tokens and $\Phi_{\text{tub}}^{\text{high}}$ is the merging operation for high-level tasks. For parallel computing, we set Υ to one constant in each batch.

For low-level generative tasks (text-to-image or image-to-image composition), the fine-grained pixel requirements make simple merging of redundant tokens infeasible. We hence divide Turbo into two modules, making its role become *merge & restore*. Specifically, before VLMs' block, Turbo calculates and records information degree between all tokens, then removes redundant tokens using a merge module Ψ_{meg} ; while after VLMs' block, Turbo restores the merged tokens with reference to information degree, using one inverse-sampling module Ψ_{inv} . Formally,

$$\mathbf{X}' = \Phi_{\text{tub}}^{\text{low}}(\mathbf{X}, \Upsilon) = \Psi_{\text{inv}}(\Psi_{\text{meg}}(\mathbf{X}, \Upsilon)) \in \mathbb{R}^{N \times D}, \quad (17)$$

Such Turbo greatly reduces computing overhead for VLMs' blocks, while ensuring pixel-level generation. Note that, in above process, we employ bipartite soft matching [3] to calculate information degree, resulting in negligible additional FLOPs. Besides, Turbo allows the bulk of computing to be done in parallel, making it friendly to modern GPU devices.

Remark. Comparing to most acceleration ideas, Turbo wins many pros. **Universality.** It performs data de-redundancy, *i.e.*, reducing computing from the source of the AI system. The resultant data can be generally adopted on various VLMs, *e.g.*, understanding/generation, multi-modality/unimodality, showing powerful compatibility. **Practicality.** It fully considers the potential data-repetition guided by semantics, accelerating with little performance loss. Besides, it's user-friendly without cumbersome tricks. **Plug-and-Play.** It works as plug-in without additional parameters for re-training, and is plain to avoid trivial development efforts.

4. Experiments

We here conduct experiments on tasks of understanding and generation across several public benchmarks.

4.1. Implementation

Understanding Benchmarks. We evaluate Turbo on unimodal Image Classification, and multi-modal tasks like

PlugIn	Performance		Ratio Υ	Acceleration	
	Dev	Test		FLOPs	Throughput
-	82.5	83.3	-	132.5	117.5
UPop	80.3	81.1	-	89.4 (-0.32 \times)	138.5 (1.18 \times)
ToMe	79.3	79.5	35	77.2 (-0.42 \times)	182.9 (1.56 \times)
Turbo	81.4	82.2	35	77.2 (-0.42 \times)	182.8 (1.56 \times)
	80.5	81.5	45	62.2 (-0.53 \times)	224.2 (1.91\times)
UPop*	79.0	79.8	35	54.7 (-0.59\times)	188.2 (1.60 \times)

Table 1. **NLVR Acceleration for BLIP on the NLVR2 dataset.** Ratio denotes the number of reduced tokens per layer and - denotes the original accuracy of BLIP model on NLVR. In UPop*, we apply Turbo to the model pruned by UPop, proving that our method is perpendicular to those model-oriented methods. Our method surpasses the other approaches by a large margin both on inference speed and accuracy.

PlugIn	Performance		Ratio Υ	Acceleration	
	Dev	Std		FLOPs	Throughput
-	77.4	77.5	-	92.1	148.1
UPop	76.3	76.3	-	65.2 (-0.30 \times)	167.8 (1.13 \times)
ToMe	74.8	74.8	40	65.7 (-0.29 \times)	184.8 (1.25 \times)
Turbo	76.8	76.9	40	65.7 (-0.29 \times)	184.6 (1.25 \times)
	76.6	76.7	60	52.5 (-0.43 \times)	232.7 (1.57\times)
UPop*	75.4	75.4	40	44.8 (-0.51\times)	206.8 (1.40 \times)

Table 2. **VQA Acceleration for BLIP on the VQAv2 dataset.** Since we adopt large models for VQA task, the drop ratio is higher than base models. By applying $ratio = 60$, we achieve the best trade-off between performance reservation and acceleration.

Cross-modal Retrieval, Natural Language for Visual Reasoning, Visual Question Answering and Image Captioning. We conduct image classification experiments on AugReg [41] and SWAG [39] models for Imagenet-1k dataset and all cross-modal tasks on BLIP [23] and BLIP2 [22] using datasets Flickr30k, COCO and NLVR2.

Generation Benchmarks. We evaluate on Stable Diffusion 1.5 [34] by generating 2000 images, each resolution is 512*512. The text classes used are from ImageNet-1k. We use FID scores to metric the generation quality.

The above experiments are conducted on one single 3090 GPU. For more details towards Turbo on different benchmarks, please refer to the supplementary materials.

4.2. Comparison with State-of-the-art

We carry out full comparisons with SOTA on both uni-modal and multi-modal VLMs, to prove the effectiveness.

Multi-Modal VLMs for Understanding. A thorough experiment on a wide range of multi-modal tasks on foundation models BLIP [23], and BLIP2 [22] are done to test the effectiveness of our method. Part of the results of understanding tasks are shown in Tables 1, 2, 3 and 4. We com-

Model	PlugIn	Performance		Acceleration	
		B@4	CIDEr	FLOPs	Throughput
BLIP	-	39.7	133.3	330.2	34.2
	UPop	38.6	128.9	137.9 (-0.58 \times)	56.6 (1.65 \times)
	ToMe	35.5	120.9	134.2 (-0.60 \times)	67.9 (1.99 \times)
	Turbo	38.2	130.0	134.2 (-0.60 \times)	67.6 (1.98 \times)
	UPop*	37.3	126.0	60.8 (-0.82\times)	74.8 (2.19\times)
BLIP2	-	42.7	145.7	1379.2	29.5
	ToMe	40.8	137.7	1029.5 (-0.25 \times)	51.1 (1.73 \times)
	Turbo	42.1	142.2	989.7 (-0.29\times)	50.9 (1.72\times)

Table 3. **Caption Acceleration on COCO.** The drop ratio is 16 and (30, 40) for Turbo on BLIP2 and BLIP respectively. CIDEr and B@4 are two standards for captioning evaluation. Turbo attains competitive performance while largely enhance throughput.

pare our method Turbo to the baseline [2] and one model-pruned based approach UPop [36]. Overall, Turbo achieves the best trade-off on acceleration rate and the performance preservation on all benchmarks. We exceed the baseline by a large margin on almost all tasks, meanwhile achieving better or competitive performance to training-required method UPop with less inference time. Compared to model-pruning methods that require further training specially designed for different models, Turbo needs no extra training and can play simple plug-in for various models. What’s more, due to the considerable cost of memory access time, FLOPs is not inversely proportional to the actual throughput. This results in a poor acceleration performance for model-pruning method on real scenarios, because these methods can’t reduce the memory access time of data. In contrast, by directly pruning data, our Turbo saves both memory access time and calculation amount.

NLVR: Table 1 demonstrates the result on NLVR task under different drop ratios Υ . Turbo performs the best even with an acceleration of 1.91 compared to 1.56 for the baseline and 1.18 for UPop. We also apply Turbo Plug-in into the model pruned by UPop (Note as UPop*). The results show that Turbo is perpendicular to the model-perspective acceleration, further reflecting the universality of Turbo.

VQA: Table 2 evaluates on the VQA task for BLIP. Turbo again exceeds the other methods either on performance or acceleration even with large drop ratios.

Image Captioning: We demonstrate the result of image captioning on both BLIP and BLIP2 in Table 3. As a difficult multi-modal task, image captioning requires fine-grained information. The baseline ToMe performs poorly on this task, dropping from 133.3 to 120.9 on CIDEr, implying a non-negligible loss of information during token merging. However, Turbo can retain much better performance to 130.0 with the same FLOPs and throughput, proving that our method can preserve more fine-grained information by encouraging aggregation of background rather than fore-

ground. We also show that turbo could further accompany model-pruning methods to get even faster inference.

Multi-modal Retrieval: Along with the image captioning, multi-modal retrieval often deal with large amount of data, *i.e.* millions or even billions of image-text pairs in real scenarios, so there is an urgent demand for inference speed-up. Table 4 demonstrates that, Turbo exceeds the baseline and model-pruning methods by a large margin on several benchmarks, *i.e.* 4.3% for image-text and 6.7% for text-image and on BLIP Flickr30k compared to UPop. With such an acceptable accuracy drop, our method is expecting to make large-scale retrieval and captioning more efficiently.

Multi-Modal Generation VLMs. Our Turbo is also suitable for fine-grained visual generation. Table 5 compares the performance-acceleration across text-to-image, image-to-image tasks. Comparing to the competitor, Turbo obtains better generation quality, *i.e.*, lower FID scores, with a an even better acceleration. While achieving similar generation results, Turbo brings significant throughput gains over vanilla stable diffusion models. Limited by paper pages, we refer the readers to the supplementary materials for detailed visualizations and ablation studies.

Uni-Modal Foundation Models. We perform uni-modal experiments on ImageNet-1k with two different training plans: AugReg [41] and SWAG [39]. Table 6 compares between our method and baseline ToMe [2]. Our Turbo surpasses ToMe on models of all sizes and training plans, while keeping the same acceleration rate. Note that image classification is rather simple comparing to multi-modal understanding tasks, so the performance drop is relatively small for the baseline. Nevertheless, Turbo achieves a thorough improvement on all uni-modal benchmarks.

4.3. Ablation Study & Discussion

We here make comprehensive ablations to dissect components. Without loss of generality, all analysis below are conducted on the BLIP image captioning task.

Effectiveness of Mutual Redundancy & Semantic Value. Mutual redundancy serves as one key component of our progressive merging strategy. As illustrated in Section 3.2, mutual redundancy reveals the hidden dependency relationship between tokens. Table 7 demonstrate the performance boost w/ and w/o mutual redundancy. By adding mutual redundancy solely or on the basis of semantic value, we can witness an obvious boost in final performance. We also study the effect of semantic value in Table 7. Similarly, semantic value also has an apparent enhancement for model performance. By balancing these two components, we launch the information degree to achieve the best results.

Trend of Key Components with Respect to Drop Ratio. In addition to the ablation study on one single drop ratio Υ , we investigate the fluctuation of performance in a wide

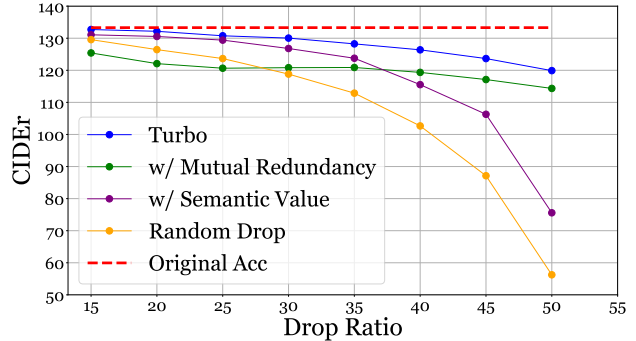


Figure 4. **Ablation Study on Drop Ratio Υ .** We evaluate separately the effectiveness of key components on various Υ . Semantic value retains superior performance when Υ is small while mutual redundancy possesses better stability on large Υ . By combining these two drop strategies, our method achieves both competitive performance and stability on the whole scope.

range of Υ . In figure 4, we demonstrate the performance of each component combination on different drop ratios. On one hand, the scheme with only mutual redundancy is relatively stable on the large scope but performs badly on small Υ . This accords with our prediction in Section 3.2 that mutual redundancy can't distinct important tokens. On account of the aggregation of semantic-rich tokens at early stages, it will inevitably lose fine-grained information. Some visualization results will be presented in supplementary materials to demonstrate this phenomenon.

On the other hand, scheme that is solely guided by semantic values possesses satisfying results on small Υ but drops dramatically on large Υ . This is due to the fact that the approximation of information degree in expression 12 only holds when the neighbourhood condition is satisfied. When drop ratio gets larger, the neighbourhood condition is no longer valid, resulting in a dramatic drop in performance. By combing semantic value with mutual redundancy, we achieve superior performance on all the scope of Υ .

Fusion for Information Degree. We mainly adopt two fusion strategies illustrated in Eq. 15. As shown in Table 7, the coupled product strategy and weighted averaging strategy achieves similar performance, further proving the robustness of the turbo module. However, due to the complexity of multiplication over addition, the coupled product strategy is slower than weighted averaging strategy. Furthermore, several complex fusion strategies *i.e.*, dynamic α on different layers are also studied. However, they all result in minor enhancement, therefore we here simply adopt the weighted averaging for efficient merging.

Framework Robustness. The balancing coefficient α in Eq. 15 is a critical hyper-parameter, which can be toxic for the framework, since we have to take time to carefully choose α if it has a vital influence on final performance.

Model	Dataset	PlugIn	Image-To-Text		Text-To-Image		Acceleration	
			R@1	R@5	R@1	R@5	FLOPs	Throughput
BLIP2 [22]	Flickr30k	-	97.6	100.0	89.7	98.1	717.5	10.7
		ToMe [2]	96.4	100.0	86.5	97.2	376.1 (-0.47X)	19.9 (+1.86X)
		Turbo	96.7_{+0.3}	100.0_{+0.0}	87.9_{+1.4}	97.4_{+0.2}	376.0 (-0.47X)	19.7 (+1.85X)
	COCO	-	85.4	97.0	68.3	87.7	717.5	10.8
		ToMe [2]	83.6	95.8	66.4	86.7	396.5 (-0.45X)	18.7 (+1.73X)
		Turbo	84.2_{+0.6}	96.2_{+0.4}	67.1_{+0.7}	87.1_{+0.4}	396.5 (-0.45X)	18.6 (+1.72X)
BLIP [23]	Flickr30k	-	97.2	99.9	87.3	97.6	55.5	281.0
		ToMe [2]	93.7	99.5	80.1	95.5	37.0 (-0.33X)	375.6 (+1.34X)
		UPop [36]	92.5	99.0	78.4	94.5	39.1 (-0.29X)	322.2 (+1.15X)
		Turbo	96.8_{+3.1}	99.8_{+0.3}	85.1_{+5.0}	96.8_{+1.3}	37.0 (-0.33X)	375.0 (+1.33X)
	COCO	-	81.9	95.4	64.3	86.1	55.5	285.0
		ToMe [2]	74.2	92.1	56.5	80.4	36.8 (-0.34X)	381.3 (+1.34X)
		UPop [36]	77.4	93.4	59.8	83.1	39.1 (-0.29X)	323.2 (+1.13X)
		Turbo	78.8_{+4.6}	94.7_{+2.6}	61.3_{+4.8}	84.2_{+3.8}	36.8 (-0.34X)	380.5 (+1.34X)
			77.5	93.8	60.5	83.7	34.1 (-0.39X)	424.3 (+1.49X)

Table 4. **Retrieval Acceleration on BLIP/BLIP2 across Flickr30K/COCO datasets.** The drop ratio is 16 and (30,40) for Turbo on BLIP2 and BLIP respectively. Turbo achieves superior results compared to other methods, with a performance drop of merely 0.4% on BLIP image-text retrieval, while other two approaches drops 3.5% and 4.7% respectively.

PlugIn	Ratio Υ	Text-To-Image		Image-To-Image	
		FID	Throughput	FID	Throughput
-	-	32.12	0.32	30.04	0.29
ToMe	10	32.80	0.39	30.69	0.37
	20	32.86	0.44	30.75	0.40
Turbo	20	32.63	0.43	30.48	0.42
	30	32.77	0.50	30.56	0.49

Table 5. **Generation Acceleration for Stable Diffusion.** Turbo wins higher generation quality (FID) or faster throughput acceleration, regardless of text-to-image or image-to-image tasks.

Model	Backbone	PlugIn	Acc	Acceleration
ViT [41]	ViT-S/16	ToMe	81.4/79.3	1.53 \times
		Turbo	81.4/ 79.9	
	ViT-B/16	ToMe	84.5/82.6	1.62 \times
		Turbo	84.5/ 83.1	
	ViT-L/16	ToMe	85.8/84.2	1.71 \times
		Turbo	85.8/ 84.6	
SWAG [39]	ViT-B/16	ToMe	85.3/84.5	1.85 \times
		Turbo	85.3/ 84.9	
	ViT-L/16	ToMe	88.1/87.7	1.98 \times
		Turbo	88.1/ 87.9	
	ViT-H/14	ToMe	88.6/88.2	1.91 \times
		Turbo	88.6/ 88.4	

Table 6. **Uni-Modal ImageNet Classification Task.** Turbo shows better results on all-size models, providing similar acceleration.

To this end, we conduct an experiment on the choice of α . We test the impact of α on image captioning for BLIP (ViT-Base and ViT-Large). Figure 5 reports the results.

	Redundancy	Semantics	Fusion	B@4	CIDER	Throughput
A1			-	34.5	112.8	73.6
A2	✓		-	35.5	120.9	70.3
A3		✓	-	36.4	123.8	67.9
A4	✓	✓	+	38.2	130.0	67.6
A5	✓	✓	\times	38.2	129.9	62.8

Table 7. **Ablation Study on Key Components.** We validate the effectiveness of each component, and compare fusion strategies.

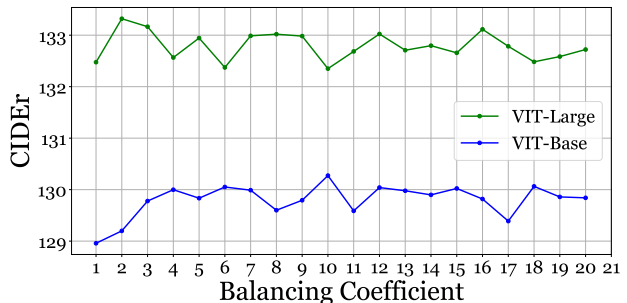


Figure 5. **Ablation Study of Balancing Coefficient.** We evaluate the influence of balancing coefficient on image captioning task using BLIP ViT-Base and ViT-Large models. The result proves the robustness of our Turbo, as the performance varies slightly in a certain range.

From the range $\alpha \in \{1, 2, \dots, 20\}$, the performance fluctuates slightly on both models with different sizes, indicating that the framework is unaware of the balancing coefficient α within a certain range. This proves our robustness.

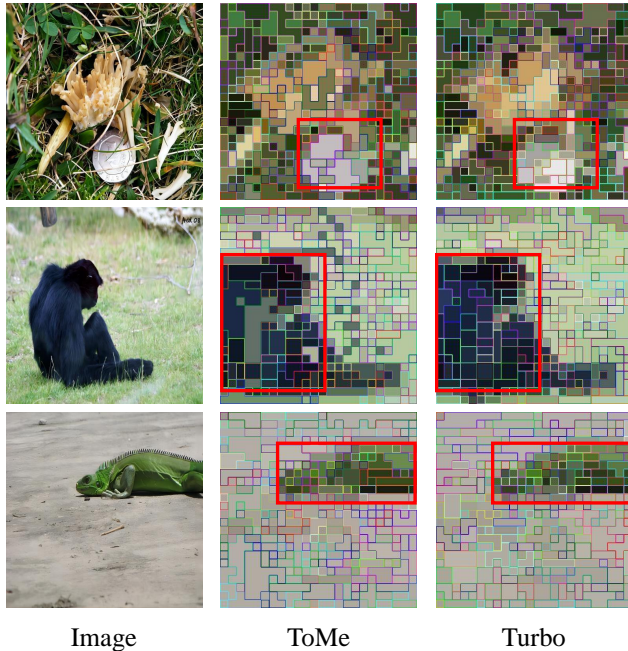


Figure 6. **Visualizations of Token Merge Process.** Turbo tends to merge background patches while retaining foreground patches with semantic value, thus preserving more critical information.

4.4. Visualization of Merging Process

As shown in Figure 6, we analyze the process of merging tokens under understanding tasks (image classification). And ToMe [2] is selected for comparisons. In each image, we highlight the foreground object in the red box. There is one clear trend that, comparing to ToMe, our Turbo merges more background patches, while retaining most foreground patches with semantic value. As a result, the data accelerated by Turbo will maintain more comprehensive and fine-grained information, ensuring higher task performance, especially on difficult tasks like image captioning and vqa.

5. Conclusion

This paper proposes Turbo plug-in for VLMs’ acceleration, from one novel perspective of data de-redundancy. In pursuit of speed-performance trade-offs, Turbo defines information degree for data reduction, taking into account two critical components: mutual redundancy and semantic value. The former evaluates data overlap between sequential tokens; the latter evaluates token’s contribution to overall semantics. By eliminating data redundancy from the source, Turbo generally compatible to various VLMs with trivial development efforts. Extensive experiments and thorough ablations show the significance of Turbo, across multi-modality/uni-modality and understanding/generation.

References

- [1] Faez Ahmed, John P Dickerson, and Mark Fuge. Diverse weighted bipartite b-matching. *arXiv preprint arXiv:1702.07134*, 2017. 12
- [2] Daniel Bolya, Cheng-Yang Fu, Xiaoliang Dai, Peizhao Zhang, Christoph Feichtenhofer, and Judy Hoffman. Token merging: Your vit but faster. *arXiv preprint arXiv:2210.09461*, 2022. 2, 4, 6, 7, 8, 9, 12
- [3] Bartłomiej Bosek, Dariusz Leniowski, Piotr Sankowski, and Anna Zych. Online bipartite matching in offline time. In *2014 IEEE 55th Annual Symposium on Foundations of Computer Science*. IEEE, 2014. 5
- [4] Tom Brown, Benjamin Mann, Nick Ryder, Melanie Subbiah, Jared D Kaplan, Prafulla Dhariwal, Arvind Neelakantan, Pranav Shyam, Girish Sastry, Amanda Askell, et al. Language models are few-shot learners. *Advances in neural information processing systems*, 33:1877–1901, 2020. 1
- [5] Xu Chen, Zida Cheng, Jiangchao Yao, Chen Ju, Weilin Huang, Jinsong Lan, Xiaoyi Zeng, and Shuai Xiao. Enhancing cross-domain click-through rate prediction via explicit feature augmentation. *arXiv preprint arXiv:2312.00078*, 2023. 2
- [6] Yen-Chun Chen, Linjie Li, Licheng Yu, Ahmed El Kholy, Faisal Ahmed, Zhe Gan, Yu Cheng, and Jingjing Liu. Uniter: Universal image-text representation learning. In *Proceedings of the European Conference on Computer Vision*. Springer, 2020. 2
- [7] Zida Cheng, Chen Ju, Xu Chen, Zhonghua Zhai, and Shuai Xiao. Image to multi-modal retrieval learning for industrial application. *arXiv preprint arXiv:2305.03972*, 2023. 2
- [8] Patrick Esser, Robin Rombach, and Bjorn Ommer. Taming transformers for high-resolution image synthesis. In *Proceedings of the IEEE/CVF conference on computer vision and pattern recognition*, pages 12873–12883, 2021. 4
- [9] Zhiyuan Fang, Jianfeng Wang, Xiaowei Hu, Lijuan Wang, Yezhou Yang, and Zicheng Liu. Compressing visual-linguistic model via knowledge distillation. In *Proceedings of the International Conference on Computer Vision*, 2021. 2
- [10] Kaiming He, Xinlei Chen, Saining Xie, Yanghao Li, Piotr Dollár, and Ross Girshick. Masked autoencoders are scalable vision learners. In *Proceedings of the IEEE Conference on Computer Vision and Pattern Recognition*, 2022. 4
- [11] Jonathan Ho, Ajay Jain, and Pieter Abbeel. Denoising diffusion probabilistic models. *Advances in Neural Information Processing Systems*, 2020. 2
- [12] Chao Jia, Yinfei Yang, Ye Xia, Yi-Ting Chen, Zarana Parekh, Hieu Pham, Quoc V. Le, Yunhsuan Sung, Zhen Li, and Tom Duerig. Scaling up visual and vision-language representation learning with noisy text supervision. In *Proceedings of the International Conference on Machine Learning*, 2021. 1, 2
- [13] Chaoya Jiang, Haiyang Xu, Chenliang Li, Ming Yan, Wei Ye, Shikun Zhang, Bin Bi, and Songfang Huang. Trips: Efficient vision-and-language pre-training with text-relevant image patch selection. In *Proceedings of the 2022 Conference on Empirical Methods in Natural Language Processing*, pages 4084–4096, 2022. 2

- [14] Chen Ju, Tengda Han, Kunhao Zheng, Ya Zhang, and Weidi Xie. Prompting visual-language models for efficient video understanding. In *Proceedings of the European Conference on Computer Vision*. Springer, 2022. 1, 2
- [15] Chen Ju, Zeqian Li, Peisen Zhao, Ya Zhang, Xiaopeng Zhang, Qi Tian, Yanfeng Wang, and Weidi Xie. Multi-modal prompting for low-shot temporal action localization. *arXiv preprint arXiv:2303.11732*, 2023. 2
- [16] Chen Ju, Haicheng Wang, Jinxiang Liu, Chaofan Ma, Ya Zhang, Peisen Zhao, Jianlong Chang, and Qi Tian. Constraint and union for partially-supervised temporal sentence grounding. *arXiv preprint arXiv:2302.09850*, 2023. 2
- [17] Chen Ju, Peisen Zhao, Siheng Chen, Ya Zhang, Yanfeng Wang, and Qi Tian. Divide and conquer for single-frame temporal action localization. In *Proceedings of the International Conference on Computer Vision*, 2021. 2
- [18] Chen Ju, Peisen Zhao, Siheng Chen, Ya Zhang, Xiaoyun Zhang, Yanfeng Wang, and Qi Tian. Adaptive mutual supervision for weakly-supervised temporal action localization. *IEEE Transactions on Multimedia*, 2022. 2
- [19] Chen Ju, Peisen Zhao, Ya Zhang, Yanfeng Wang, and Qi Tian. Point-level temporal action localization: Bridging fully-supervised proposals to weakly-supervised losses. *arXiv preprint arXiv:2012.08236*, 2020. 2
- [20] Chen Ju, Kunhao Zheng, Jinxiang Liu, Peisen Zhao, Ya Zhang, Jianlong Chang, Qi Tian, and Yanfeng Wang. Distilling vision-language pre-training to collaborate with weakly-supervised temporal action localization. In *Proceedings of the IEEE Conference on Computer Vision and Pattern Recognition*, 2023. 2
- [21] Wonjae Kim, Bokyung Son, and Ildoo Kim. Vilt: Vision-and-language transformer without convolution or region supervision. In *Proceedings of the International Conference on Machine Learning*. PMLR, 2021. 1, 2
- [22] Junnan Li, Dongxu Li, Silvio Savarese, and Steven Hoi. Blip-2: Bootstrapping language-image pre-training with frozen image encoders and large language models. *arXiv preprint arXiv:2301.12597*, 2023. 1, 2, 6, 8
- [23] Junnan Li, Dongxu Li, Caiming Xiong, and Steven Hoi. Blip: Bootstrapping language-image pre-training for unified vision-language understanding and generation. In *International Conference on Machine Learning*, pages 12888–12900. PMLR, 2022. 1, 2, 5, 6, 8
- [24] Jinxiang Liu, Chen Ju, Chaofan Ma, Yanfeng Wang, Yu Wang, and Ya Zhang. Audio-aware query-enhanced transformer for audio-visual segmentation. *arXiv preprint arXiv:2307.13236*, 2023. 2
- [25] Jinxiang Liu, Chen Ju, Weidi Xie, and Ya Zhang. Exploiting transformation invariance and equivariance for self-supervised sound localisation. In *Proceedings of ACM International Conference on Multimedia*, 2022. 2
- [26] Jinxiang Liu, Yu Wang, Chen Ju, Ya Zhang, and Weidi Xie. Annotation-free audio-visual segmentation. *arXiv preprint arXiv:2305.11019*, 2023. 2
- [27] Huaishao Luo, Lei Ji, Ming Zhong, Yang Chen, Wen Lei, Nan Duan, and Tianrui Li. Clip4clip: An empirical study of clip for end to end video clip retrieval and captioning. *Neurocomputing*, 2022. 2
- [28] Chaofan Ma, Yuhuan Yang, Chen Ju, Fei Zhang, Jinxiang Liu, Yu Wang, Ya Zhang, and Yanfeng Wang. Diffusionseg: Adapting diffusion towards unsupervised object discovery. *arXiv preprint arXiv:2303.09813*, 2023. 2
- [29] Chaofan Ma, Yuhuan Yang, Chen Ju, Fei Zhang, Ya Zhang, and Yanfeng Wang. Open-vocabulary semantic segmentation via attribute decomposition-aggregation. *arXiv preprint arXiv:2309.00096*, 2023. 2
- [30] Ron Mokady, Amir Hertz, and Amit H Bermano. Clip-cap: Clip prefix for image captioning. *arXiv preprint arXiv:2111.09734*, 2021. 2
- [31] Alec Radford, Jong Wook Kim, Chris Hallacy, Aditya Ramesh, Gabriel Goh, Sandhini Agarwal, Girish Sastry, Amanda Askell, Pamela Mishkin, Jack Clark, Gretchen Krueger, and Ilya Sutskever. Learning transferable visual models from natural language supervision. In *Proceedings of the International Conference on Machine Learning*, 2021. 1, 2
- [32] Aditya Ramesh, Prafulla Dhariwal, Alex Nichol, Casey Chu, and Mark Chen. Hierarchical text-conditional image generation with clip latents. *arXiv preprint arXiv:2204.06125*, 2022. 2
- [33] Yongming Rao, Wenliang Zhao, Benlin Liu, Jiwen Lu, Jie Zhou, and Cho-Jui Hsieh. Dynamicvit: Efficient vision transformers with dynamic token sparsification. *Advances in Neural Information Processing Systems*, 2021. 2
- [34] Robin Rombach, Andreas Blattmann, Dominik Lorenz, Patrick Esser, and Björn Ommer. High-resolution image synthesis with latent diffusion models. In *Proceedings of the IEEE/CVF conference on computer vision and pattern recognition*, pages 10684–10695, 2022. 1, 2, 6, 12
- [35] Sheng Shen, Zhen Dong, Jiayu Ye, Linjian Ma, Zhewei Yao, Amir Gholami, Michael W Mahoney, and Kurt Keutzer. Q-bert: Hessian based ultra low precision quantization of bert. In *Proceedings of the AAAI Conference on Artificial Intelligence*, 2020. 1, 2
- [36] Dachuan Shi, Chaofan Tao, Ying Jin, Zhendong Yang, Chun Yuan, and Jiaqi Wang. Upop: Unified and progressive pruning for compressing vision-language transformers. *arXiv preprint arXiv:2301.13741*, 2023. 2, 6, 8
- [37] Dachuan Shi, Chaofan Tao, Anyi Rao, Zhendong Yang, Chun Yuan, and Jiaqi Wang. Crossget: Cross-guided ensemble of tokens for accelerating vision-language transformers. *arXiv preprint arXiv:2305.17455*, 2023. 2
- [38] Zhan Shi, Xu Zhou, Xipeng Qiu, and Xiaodan Zhu. Improving image captioning with better use of captions. *arXiv preprint arXiv:2006.11807*, 2020. 2
- [39] Mannat Singh, Laura Gustafson, Aaron Adcock, Vinicius de Freitas Reis, Bugra Gedik, Raj Prateek Kosaraju, Dhruv Mahajan, Ross Girshick, Piotr Dollár, and Laurens Van Der Maaten. Revisiting weakly supervised pre-training of visual perception models. In *Proceedings of the IEEE/CVF Conference on Computer Vision and Pattern Recognition*, pages 804–814, 2022. 6, 7, 8
- [40] Haoyu Song, Li Dong, Wei-Nan Zhang, Ting Liu, and Furu Wei. Clip models are few-shot learners: Empirical studies on vqa and visual entailment. *arXiv preprint arXiv:2203.07190*, 2022. 2

- [41] Andreas Steiner, Alexander Kolesnikov, Xiaohua Zhai, Ross Wightman, Jakob Uszkoreit, and Lucas Beyer. How to train your vit? data, augmentation, and regularization in vision transformers. *arXiv preprint arXiv:2106.10270*, 2021. [6](#), [7](#), [8](#)
- [42] Aaron Van Den Oord, Oriol Vinyals, et al. Neural discrete representation learning. *Advances in neural information processing systems*, 30, 2017. [4](#)
- [43] Tiannan Wang, Wangchunshu Zhou, Yan Zeng, and Xinsong Zhang. Efficientvlm: Fast and accurate vision-language models via knowledge distillation and modal-adaptive pruning. *arXiv preprint arXiv:2210.07795*, 2022. [1](#), [2](#)
- [44] Zekun Wang, Jingchang Chen, Wangchunshu Zhou, Ming Liu, and Bing Qin. Smarttrim: Adaptive tokens and parameters pruning for efficient vision-language models. *arXiv preprint arXiv:2305.15033*, 2023. [2](#)
- [45] Jason Wei, Yi Tay, Rishi Bommasani, Colin Raffel, Barret Zoph, Sebastian Borgeaud, Dani Yogatama, Maarten Bosma, Denny Zhou, Donald Metzler, et al. Emergent abilities of large language models. *arXiv preprint arXiv:2206.07682*, 2022. [1](#)
- [46] Yuhuan Yang, Chaofan Ma, Chen Ju, Ya Zhang, and Yanfeng Wang. Multi-modal prototypes for open-set semantic segmentation. *arXiv preprint arXiv:2307.02003*, 2023. [2](#)
- [47] Peisen Zhao, Lingxi Xie, Chen Ju, Ya Zhang, Yanfeng Wang, and Qi Tian. Bottom-up temporal action localization with mutual regularization. In *Proceedings of the European Conference on Computer Vision*. Springer, 2020. [2](#)
- [48] Kaiyang Zhou, Jingkang Yang, Chen Change Loy, and Ziwei Liu. Learning to prompt for vision-language models. *International Journal of Computer Vision*, 2022. [1](#)
- [49] Deyao Zhu, Jun Chen, Xiaoqian Shen, Xiang Li, and Mohamed Elhoseiny. Minigt-4: Enhancing vision-language understanding with advanced large language models. *arXiv preprint arXiv:2304.10592*, 2023. [2](#)

In the supplementary material, we first provide more details about our plug-in turbo module to facilitate reproduction. Then more ablation studies on different fusion strategies are provided. Finally we demonstrate some visualization results to justify our arguments, including the generated images from stable diffusion and intermediate merging process of understanding tasks.

6. Implementation Details

6.1. Turbo Architecture for Understanding Tasks

Turbo can be easily plugged in almost any pre-trained, attention-based models to reduce the total sequence length block by block, with no need for further training or adjustment. In practice, we replace all the attention blocks by the turbo module.

For Turbo, we merge tokens progressively based on their information degree, which is defined as follows:

$$\mathcal{E} = \mathcal{R} - \alpha\mathcal{I}, \quad \mathcal{E} = \frac{\mathcal{R}}{\mathcal{I}}. \quad (18)$$

Information degree takes both mutual redundancy and semantic values into account, encouraging insignificant, similar tokens to be merged preferentially. This merging strategy reduces the amount of tokens with duplicated or low informativity, compressing the token sequence with minor information loss. Inspired by [1,2], we follow the bipartite soft matching to calculate mutual redundancy and apply the merging strategy to aggregate tokens. Specifically, we leverage keys (K) or queries (Q) in QKV attention and the cosine similarity metric between tokens to measure the similarity between tokens. We define mutual redundancy between two tokens as the similarity between them. By adding the quantity of semantic value, which is the attention proportion of each token, the information degree is obtained.

To avoid excessive computational cost of calculating similarity matrix of the whole token sequence, we leverage bipartite soft matching to speed up the merging process. Suppose the drop ratio is Υ , which means we will reduce the amount of tokens by number Υ in each block. In every block, we divide the tokens into two partitions B and C of the same size (if the number of tokens is odd, one partition has 1 more tokens than the other). Then we calculate the mutual redundancy between the two partitions B and C . After adding the semantic value of each token on partition B , we sort the information degree of B and merge the top Υ tokens onto C . At last we concatenate the sequence back to continue the forwarding process. In this way, we reduce the length of token sequence by Υ in each block. Notice that We call Υ the drop ratio, but it is in fact the number of tokens we reduce every attention block, which is a real ratio by dividing the length of the token sequence. We also note that the semantic value are naturally contained in vi-

sual cls self-attention map or texture cls cross-attention map depending on the model structure.

When the merging process are finished, some tokens can represent several different patches. This can change the outcome of softmax attention and thus influence the semantic value. So We fix this with a minor modification:

$$\mathbf{A} = \text{softmax} \left(\frac{QK^T}{\sqrt{d}} + \log s \right), \quad (19)$$

where s is the number of patches/tokens represented by the merged tokens all along the merging procedure.

In order to avoid excessive merging, *i.e.*, merging too many tokens and leave only a few tokens in final blocks. This will cause insufficient expression ability problem and we observe a sharp performance drop at certain drop ratio. So we set up a threshold r for the least number of tokens in the final stage, to mitigate the dramatic drop on large Υ . Table 9 shows the effectiveness of this restriction for preventing a sudden performance decline.

6.2. Turbo Architecture for Generation Tasks

For low-level generative tasks, Stable Diffusion [34] is one popular backbone. Here, Turbo contains one merging module and one inverse-sampling module. For the merging module, we attach Turbo acceleration on UNet of Stable Diffusion, as UNet consumes the most computation. More specifically, UNet usually consists of three key components: self-attention, cross-attention and FFN. We add Turbo merging/restoring before/ after each component. For self-attention and FFN, Turbo merging is calculated by one visual modality; while for cross-attention, Turbo merging is calculated by visual-textual modalities.

We evaluate by generating 2000 images, each resolution is $512 * 512$. The text classes used are from ImageNet-1k. We use FID scores to metric the generation quality.

7. More Experiments

7.1. Ablation Study on Fusion Strategy

We design 4 different fusion strategies to combine mutual redundancy (\mathcal{R}) with semantic value (\mathcal{I}):

$$S1 : \mathcal{E} = \mathcal{R} - \alpha\mathcal{I}, \quad (20)$$

$$S2 : \mathcal{E} = \frac{\mathcal{R}}{\mathcal{I}}, \quad (21)$$

$$S3 : \mathcal{E} = \mathcal{R}(1 - \alpha\mathcal{I}), \quad (22)$$

$$S4 : \mathcal{E} = \mathcal{R} - \beta^{|\gamma - \text{block.id}|} \alpha\mathcal{I}, \quad (23)$$

where S4 is designed to allow dynamic scales between \mathcal{R} and \mathcal{I} on different blocks. For example, if $\beta > 1$ and $\gamma = 6$, then the scale of \mathcal{I} will reach its maximum on block 6 and attain the minimum value on two-end blocks.

Strategy	α	β	γ	B@4	CIDEr	Throughput
S1	6	-	-	38.2	130.0	67.6
S2	-	-	-	38.2	129.9	62.8
S3	1	-	-	37.8	128.5	61.9
S3	2	-	-	37.9	128.4	61.9
S3	3	-	-	36.9	125.7	61.9
S3	4	-	-	36.1	123.1	61.9
S4	6	0.9	1	38.2	129.5	67.4
S4	6	0.9	2	38.3	129.5	67.4
S4	6	0.9	3	38.1	129.5	67.4
S4	6	0.9	4	38.2	129.5	67.4
S4	6	0.9	5	38.1	129.7	67.4
S4	6	0.9	6	38.0	129.2	67.4
S4	6	0.9	7	38.0	129.5	67.4
S4	6	0.9	8	38.4	130.2	67.4
S4	6	0.9	9	38.2	129.9	67.4
S4	6	0.9	10	38.2	129.7	67.4
S4	6	1.1	1	38.3	130.0	67.4
S4	6	1.1	2	38.3	130.3	67.4
S4	6	1.1	3	38.4	130.1	67.4
S4	6	1.1	4	38.3	129.9	67.4
S4	6	1.1	5	38.5	129.9	67.4
S4	6	1.1	6	38.1	129.3	67.4
S4	6	1.1	7	38.2	129.6	67.4
S4	6	1.1	8	38.5	130.3	67.4
S4	6	1.1	9	38.2	129.8	67.4
S4	6	1.1	10	38.2	129.6	67.4

Table 8. **Ablation Study on Fusion Strategies.** We adopt several fusion strategies and test their performance under different coefficients. Some complex fusion strategies can achieve slightly better results, but in order to keep the form easy to apply, we adopt the simple weighted average in other experiments.

Υ	Threshold	B@4	CIDEr	Throughput
65	0	28.8	95.5	107.6
65	70	31.1	104.3	103.3
65	130	34.2	115.3	100.8
70	0	27.3	89.4	113.0
70	70	31.0	103.7	110.7

Table 9. **Ablation Study on Threshold.** We validate the effectiveness of threshold to prevent dramatic performance drop on large Υ . With slight decline on speed, model performance with threshold on minimum token length can maintain a smoother decrease when Υ getting larger.

As shown in table 8, we have done extensive experiments on the four fusion strategies with different coefficients. Though S4 attains the best result, due to its complexity and such slight performance gain, *i.e.*, three hyperparameters to be determined with a gain of only 0.3 on CIDEr, we thus adopt the simple weighted average fusion strategy (S1) on our turbo module.

7.2. Ablation Study on Threshold

When applying large drop ratios Υ on turbo module, we witness a sharp drop of model performance. We argue that this phenomenon is due to the insufficient expression ability of token sequence length below a certain threshold. So

we append a threshold on minimum number of tokens left in the final block. Specifically, we stop the token merging process once the token sequence length is below the threshold. Results in table 9 have demonstrate the effectiveness of such a threshold on large Υ , improving the model performance by over 10 points on CIDEr with slight acceleration declines.